Journal of Photochemistry and Photobiology A: Chemistry 244 (2012) 54–64

Contents lists available at SciVerse ScienceDirect

Journal of Photochemistry and Photobiology A: Chemistry

journal homepage: www.elsevier.com/locate/jphotochem

Synthesis, characterization and photochromism of 3′-butoxyflavylium derivatives

Sandra Gago, Vesselin Petrov, A. Jorge Parola, Fernando Pina*

REQUIMTE, Departamento de Química, Faculdade de Ciências e Tecnologia, Universidade Nova de Lisboa, 2829-516 Monte de Caparica, Portugal

ARTICLE INFO

Article history:
Received 1 May 2012
Received in revised form 6 June 2012
Accepted 16 June 2012
Available online 10 July 2012

Keywords:
Flavylium compounds
Photochromic
Anthocyanins
Flash photolysis

ABSTRACT

The compounds 3′-butoxy-7-methoxyflavylium and 3′-butoxy-7-hydroxyflavylium were synthesized and the respective equilibrium and rate constants determined by two complementary techniques, pH jumps and flash photolysis. An experimental strategy based on these two techniques allowed calculation of all the equilibrium and rate constants of the system carried out for the first time in flavylium compounds lacking of the high *cis*–*trans* isomerization barrier. Irradiation of the *trans*-chalcone gives rise to the formation of the *cis*-chalcone still during the lifetime of the flash, which disappears through two parallel reactions: (i) one leading to the recovery of the *trans*-chalcone and the other, (ii) forming flavylium cation via hemiketal. This last reaction is globally dependent on pH and at less acidic pH the system reverts back to the *trans*-chalcone. The highest yield of colour production upon the flash takes place in the pH range 2–3.5.

1. Introduction

Photochromic compounds, which have the property of changing their colour upon light absorption and revert thermally to the initial state, seem to be magic and always fascinating [1]. In recent years, a new family of photochromic compounds derived from 2-phenyl-1-benzopyrylium, the so-called synthetic flavylium compounds, have been reported in literature [2,3]. Synthetic flavylium compounds possess the same basic structure of anthocyanins, the ubiquitous colorants of most flowers and fruits and follow together with deoxyanthocyanins [4–7] styrylflavylium [8–12] and naphthoflavylium analogues [13,14], the same network of chemical reactions. The flavylium cation (red in anthocyanins), is stable only at very acidic pH values. As the pH is raised, other species are formed in a more or less complex kinetic process, the respective details being very dependent on the substitution pattern of the flavylium backbone.

When sufficiently acidic solutions containing flavylium cations bearing hydroxyl substituents are made less acidic by addition of base (pH jumps), the first observation is the appearance of a different colour due to the deprotonation of the hydroxyl group to form a quinoidal base, see Eq. (1) where this is exemplified for 4′,7-dihydroxyflavylium. All anthocyanins possess hydroxyl groups and deprotonation usually leads to the appearance of blue coloured quinoidal bases.

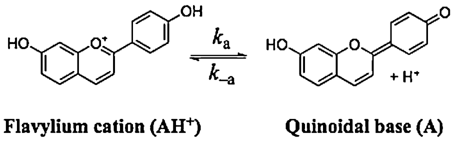

$$K_a = \frac{k_a}{k_{-a}} \quad \text{(deprotonation)} \tag{1}$$

In competition with this reaction the hydration of the flavylium cation by water addition at position 2 takes place, Eq. (2)

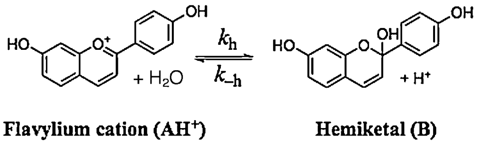

$$K_h = \frac{k_h}{k_{-h}} \quad \text{(hydration)} \tag{2}$$

These two parallel reactions occur in different scales of time: proton transfer in the micro-second and hydration in seconds to sub-seconds, depending on pH. By consequence **A** appears as a

---

* Corresponding author. Tel.: +351 212948355; fax: +351 212948550.
E-mail address: fp@fct.unl.pt (F. Pina).

1010-6030/$ – see front matter © 2012 Elsevier B.V. All rights reserved.
http://dx.doi.org/10.1016/j.jphotochem.2012.06.013

kinetic product that usually fades with time, because it is not the most stable species at the equilibrium.

The hemiketal (chromene) is involved in a tautometic process that leads to the ring opening with formation of a *cis*-chalcone form. This reaction usually occurs in the sub-second timescale.

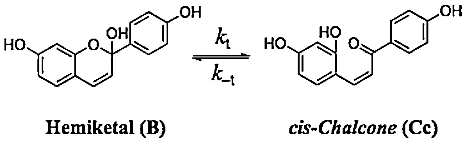

$$K_t = \frac{k_t}{k_{-t}} \qquad \text{(tautomerization)} \qquad (3)$$

Finally the *cis*-chalcone isomerizes and gives the *trans*-chalcone, in the time scale of seconds or many days depending on the *cis–trans* isomerization barrier.

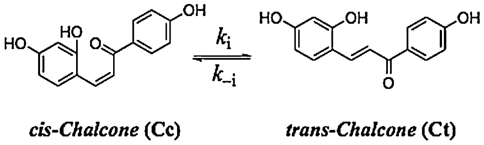

$$K_i = \frac{k_i}{k_{-i}} \qquad \text{(isomerization)} \qquad (4)$$

The photochemistry arises from the photoinduced isomerization of the *trans*-chalcone to the *cis*-chalcone, which at moderately acidic pH values is spontaneously transformed into the flavylium cation or the quinoidal base (if hydroxyl substituents are present) [2,15].

Eqs. (1)–(4) of the flavylium network are equivalent to a global acid–base equilibrium defined by Eqs. (5) and (6), where CB refers to all species formed from **A**H⁺, Eq. (7). Under these conditions, the apparent acidity constant pK'_a relates with the equilibrium constants of equilibria (1)–(4) through Eq. (8) [16–18].

$$AH^+ + 2H_2O \rightleftharpoons \mathbf{CB} + H_3O^+ \qquad (5)$$

$$K'_a = \frac{[CB][H_3O^+]}{[AH^+]} \qquad (6)$$

$$[\mathbf{CB}] = [\mathbf{Ct}] + [\mathbf{Cc}] + [\mathbf{B}] + [\mathbf{A}] \qquad (7)$$

$$K'_a = K_a + K_h + K_hK_t + K_hK_tK_i \qquad (8)$$

It is very useful to define a pseudo-equilibrium, a transient state that is obtained when all the species are in (pseudo)equilibrium except *trans*-chalcone due to its slower formation in comparison with all the other kinetic steps, Eqs. (9)–(11).

$$\mathbf{AH}^+ + 2H_2O \rightleftharpoons \mathbf{CB}^\wedge + H_3O^+ \qquad (9)$$

$$K^\wedge_a = \frac{[\mathbf{CB}^\wedge][H_3O^+]}{[\mathbf{AH}^+]} \qquad (10)$$

$$[\mathbf{CB}^\wedge] = [\mathbf{Cc}] + [\mathbf{B}] + [\mathbf{A}] \qquad (11)$$

$$K^\wedge_a = K_a + K_h + K_hK_t \qquad (12)$$

The determination of the thermodynamic and kinetic constants of the network of chemical reactions is carried out by changing the equilibrium conditions from one state to another and follow the relaxation of the system, generally by UV–vis or ^{1}H NMR. In some cases, as in the present compounds, the system is photochromic and a great profit can be taken from transient absorption measurements (flash photolysis). Once the equilibrium constants determined, an energy level diagram (as the ones reported in Schemes 2 and 3) can be obtained as well as the pH dependent mole fraction distribution of species according to Eq. (13) [19].

$$\chi_{AH^+} = \frac{[H^+]}{[H^+] + K'_a};\quad \chi_A = \frac{K'_a}{[H^+] + K'_a};\quad \chi_B = \frac{K_h}{[H^+] + K'_a};$$
$$\chi_{Cc} = \frac{K_hK_t}{[H^+] + K'_a};\quad \chi_{Ct} = \frac{K_hK_tK_i}{[H^+] + K'_a} \qquad (13)$$

In spite of the fact that practically all flavylium compounds follow the general network of chemical reactions above described there are many differences on the mole fraction distribution of species at the equilibrium and pseudo-equilibrium as well as on the rates of conversion between the species, which are very dependent on the substitution pattern [2]. Many flavylium compounds proved to be versatile photochromic systems with potential applications in solution [2] or incorporated in polymers [20], gels [21] and ionic liquids [22]; in particular, those possessing a high *cis–trans* isomerization barrier have been claimed as models for optical memories [23]. In this work, the effect of the substituents in position 3′ in the performance of the photochromic system is reported. Preliminary results suggested that the apparent acidity of the flavylium cation in these compounds is very low, meaning that it is possible to have the photoactive *trans*-chalcone species at low pH values, enlarging the operational pH range of the photochromic system [24]. Two 3′-butoxyflavylium derivatives (Scheme 1) were synthesized and studied by conjugation of pH jumps and flash photolysis. The use of both techniques allowed to calculate with good accuracy all the rate and equilibrium constants of both flavylium chemical reaction networks, Eqs. (1)–(5). In particular flash photolysis has been employed to characterize the flavylium photochromism but it is the first time that is used extensively in a strategy that allows the calculation of all the rate and equilibrium constants of the network for compounds lacking the *cis–trans* isomerization barrier.

2. Experimental

2.1. General

All reagents and solvents were of analytical grade. ^{1}H and 2D ^{1}H COSY NMR spectra were recorded at 400.13 MHz with a Bruker AMX400. The flavylium salts were dissolved in CD_3OD, acidified with DCl or basified with NaOD. The assignments of the several protons were based on the COSY experiments. Elemental analyses (EA) were performed in a Thermofinnigan Flash EA 112 series. Mass spectra were run on an Applied Biosystems Voyager-DE^{TM} PRO. Spectroscopic experiments were carried out in buffered [25] water/ethanol, 70:30 (v/v) solvent mixture. pH values were adjusted by the addition of a 0.1 M NaOH aqueous solution or a 0.1 M HCl aqueous solution, and measured with a MeterLab pHM240 pH meter from Radiometer Copenhagen. For solutions with HCl concentration above 0.1 M, pH was calculated from −log [HCl]. UV/Vis absorption spectra were recorded with a Varian-Cary 100 Bio spectrophotometer or in a Shimadzu VC2501-PC. The stopped flow experiments were conducted in an Applied

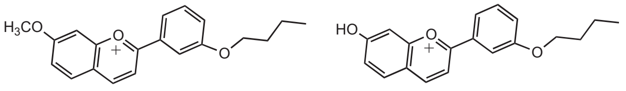

Scheme 1. Structures of 3′-butoxy-7-methoxyflavylium and 3′-butoxy-7-hydroxyflavylium.

Photophysics SX20 stopped-flow spectrometer provided with a PDA.1/UV photodiode array detector. Irradiation experiments were carried out on a spectrofluorimeter Spex Fluorolog 1681 at the wavelength 377 nm without slits. Light intensity was measured by ferrioxalate actinometry [26]. The flash photolysis experiments were performed on a Varian Cary 5000 spectrophotometer with a Harrick FiberMate attached to the CUV-ALL-UV 4-way cuvette holder compartment (Ocean Optics) on the external side of the sample holder in order to perform light excitation perpendicular to the analyzing beam and with the sample compartment shielded with black cardboard and black tape. As a pulsed light source a commercially available Achiever 630AF camera flash was used, placed in close contact with the sample holder. The excitation was made with the white light of the camera flash with a time resolution of ca. 0.05 s. Further details are described elsewhere [27].

2.2. Synthesis of 3′-butoxyacetophenone (this procedure was adapted from Refs. [28,29])

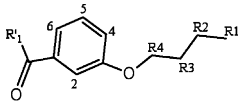

A mixture of 3′-hydroxyacetophenone (1.0 g, 7.3 mmol), 1.5 equivalents of chlorobutane (1.01 g, 10.9 mmol), 3 equivalents of potassium carbonate (3.03 g, 21.9 mmol) and a catalytic amount of potassium iodide (0.10 g) in dry DMF (20 mL) was heated at 90 °C overnight, under inert atmosphere. In the following day the reaction was monitored by TLC (ethyl acetate:hexane, 2:8) and addition of chlorobutane was needed. After completion of the reaction, the mixture was cooled to room temperature, filtered and the resulting solution combined with water (20 mL) and extracted with ethyl acetate (4 × 20 mL). The organic phase was washed with water (3 × 15 mL), dried over anhydrous sodium sulphate, filtered and the solvent removed on a rotary evaporator. A yellow oil was obtained and purified by column chromatography on silica gel (Yield: 1.26 g, 90%).

^{1}H RMN ($CDCl_3$, 400.13 MHz, 298 K) δ (ppm): 7.50 (1H, d, ^3J = 7.3 Hz), 7.47 (1H, s), 7.34 (1H, t, ^3J = 15 Hz), 7.09 (1H, d, ^3J = 6.8 Hz), 3.99 (2H, t, R4), 2.58 (3H, s, R′1); 1.77 (2H, q, R3), 1.49 (2H, q, R2), 0.97 (3H, t, R1).

2.3. Synthesis of 3′-butoxy-7-hydroxyflavylium hydrogensulphate

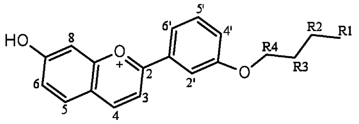

A solution of 3′-hydroxyacetophenone (0.5 g, 2.6 mmol) with one equivalent of 2,4-dihydroxybenzaldehyde (0.36 g) in a mixture of glacial acetic acid/concentrated sulphuric acid (4 mL:1 mL) was stirred overnight at room temperature. Diethyl ether was added to the red solution and a precipitate was formed. This dark yellow solid was filtered, washed several times with diethyl ether and dried under vacuum. Yield: 0.70 g, 69%. ^{1}H RMN (CD_3OD + DCl, 400.13 MHz, 298 K) δ (ppm): 9.33 (1H, H4, d, ^3J = 8.4 Hz), 8.51 (1H, H3, d, ^3J = 8.4 Hz), 8.29 (1H, H5, d, ^3J = 9.2 Hz), 8.06 (1H, H6′, d, ^3J = 7.6 Hz), 7.95 (1H, H2′, s), 7.67 (1H, H8, s); 7.64 (1H, H5′, t, ^3J = 8.0 Hz), 7.53 (1H, H6, dd, ^3J = 9.0 Hz, ^4J = 2.2 Hz), 7.40 (2H, H4′, dd, ^3J = 8.0 Hz, ^4J = 2.4 Hz), 4.18 (2H, t, R4), 1.83 (2H, m, R3), 1.56 (2H, m, R2), 1.02 (3H, t, R1); MALDI-TOF/MS: m/z (%): calcd for $C_{19}H_{19}O_3^+$: 295.13; found: 295.11 [M$^+$] (100%); Elemental analysis (%) calcd for $C_{19}H_{19}O_3 \cdot HSO_4$: C 58.15, H 5.14; found: C 58.28, H 5.17.

2.4. trans-Chalcone of 3′-butoxy-7-hydroxyflavylium hydrogensulphate

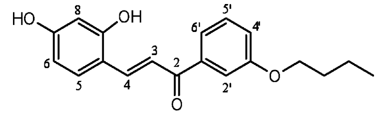

Dissolving 3′-butoxy-7-hydroxyflavylium hydrogensulphate in CD_3OD with a drop of D_2O and allowing equilibration overnight, in the dark, leads to a mixture containing >80% Ct. ^{1}H RMN (CD_3OD, pD ≈ 2.5, 400.13 MHz, 298 K) δ (ppm): 8.00 (1H, H4, d, ^3J = 15.6 Hz), 7.58 (1H, H5′, dd, ^3J = 3.8 Hz), 7.56 (1H, H3, d, ^3J = 15.6 Hz), 7.52 (1H, H5, d, ^3J = 8.4 Hz), 7.48 (1H, H2′, s), 7.45 (1H, H6′, d, ^3J = 8.0 Hz), 7.18 (1H, H4′, dd, ^3J = 8.4 Hz, ^4J = 2.0 Hz), 6.37 (2H, H6 + H8, m), 4.08 (2H, t, R4), 1.82 (2H, m, R3), 1.57 (2H, m, R2), 1.04 (3H, m, R1).

2.5. Synthesis of 3′-butoxy-7-methoxyflavylium hydrogensulphate

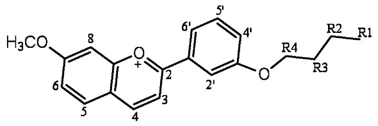

This compound was prepared as described above but using 2-hydroxy-4-methoxybenzaldehyde instead of 2,4-dihydroxybenzaldehyde. Yield: 0.87 g, 83%, dark orange solid. ^{1}H RMN (CD_3OD + DCl, 400.13 MHz, 298 K) δ (ppm): 9.35 (1H, H4, d, ^3J = 8.4 Hz), 8.55 (1H, H3, d, ^3J = 8.4 Hz), 8.28 (1H, H5, d, ^3J = 9.2 Hz), 8.07 (1H, H6′, d, ^3J = 8.0 Hz), 7.93 (1H, H2′, s), 7.90 (1H, H8, s); 7.69 (1H, H5′, dd, ^3J = 10.0 Hz), 7.60 (1H, H6, dd, ^3J = 9.2 Hz, ^4J = 1.6 Hz), 7.40 (2H, H4′, dd, ^3J = 8.4 Hz, ^4J = 1.6 Hz), 4.18 (2H, t, R4), 1.83 (2H, m, R3), 1.56 (2H, m, R2), 1.02 (3H, t, R1); MALDI-TOF/MS: m/z (%): calcd for $C_{20}H_{21}O_3^+$: 309.15; found: 309.11 [M$^+$] (100%). The compound was recrystallized in the perchlorate form for elemental analysis purpose, by dissolving in the minimum amount of ethanol and adding perchloric acid to precipitate the product. The red solid obtained was filtered off and washed several times with diethyl ether. Elemental analysis (%) calcd for $C_{20}H_{21}O_3 \cdot ClO_4$: C 58.76, H 5.18; found: C 58.89, H 5.25.

2.6. trans-Chalcone of 3′-butoxy-7-methoxyflavylium

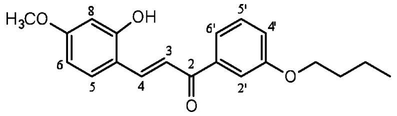

Dissolving 3′-butoxy-7-hydroxyflavylium hydrogensulphate in CD_3OD with a drop of D_2O and allowing equilibration overnight, in the dark, leads to a mixture containing >98% Ct. ^{1}H RMN (CD_3OD, pD ≈ 3.5, 400.13 MHz, 298 K) δ (ppm): 7.99 (1H, H4, d, ^3J = 15.8 Hz), 7.60 (1H, H5, d, ^3J = 8.8 Hz), 7.58 (1H, H3, d, ^3J = 15.8 Hz), 7.57 (1H, H5′, dd, ^3J = 8.0 Hz), 7.48 (1H, H6′, d, ^3J = 8.0 Hz), 7.43 (1H, H2′, s), 7.20 (1H, H4′, dd, ^3J = 7.6 Hz), 6.55 (1H, H6, dd, ^3J = 8.8 Hz), 6.50 (1H, H8, d), 4.06 (2H, t, R4), 3.82 (1H, s, OCH_3), 1.76 (2H, m, R3), 1.48 (2H, m, R2), 0.96 (3H, t, R1).

3. Results and discussion

3.1. 3′-Butoxy-7-methoxyflavylium

The absorption spectra of equilibrated solutions of the compound 3′-butoxy-7-methoxyflavylium in ethanol:water (30:70), in the dark, are shown in Fig. 1A for the pH range 2 M (HCl) < pH < 4.97 and in Fig. 1B for 3.30 < pH < 10.75. At lower pH values, the

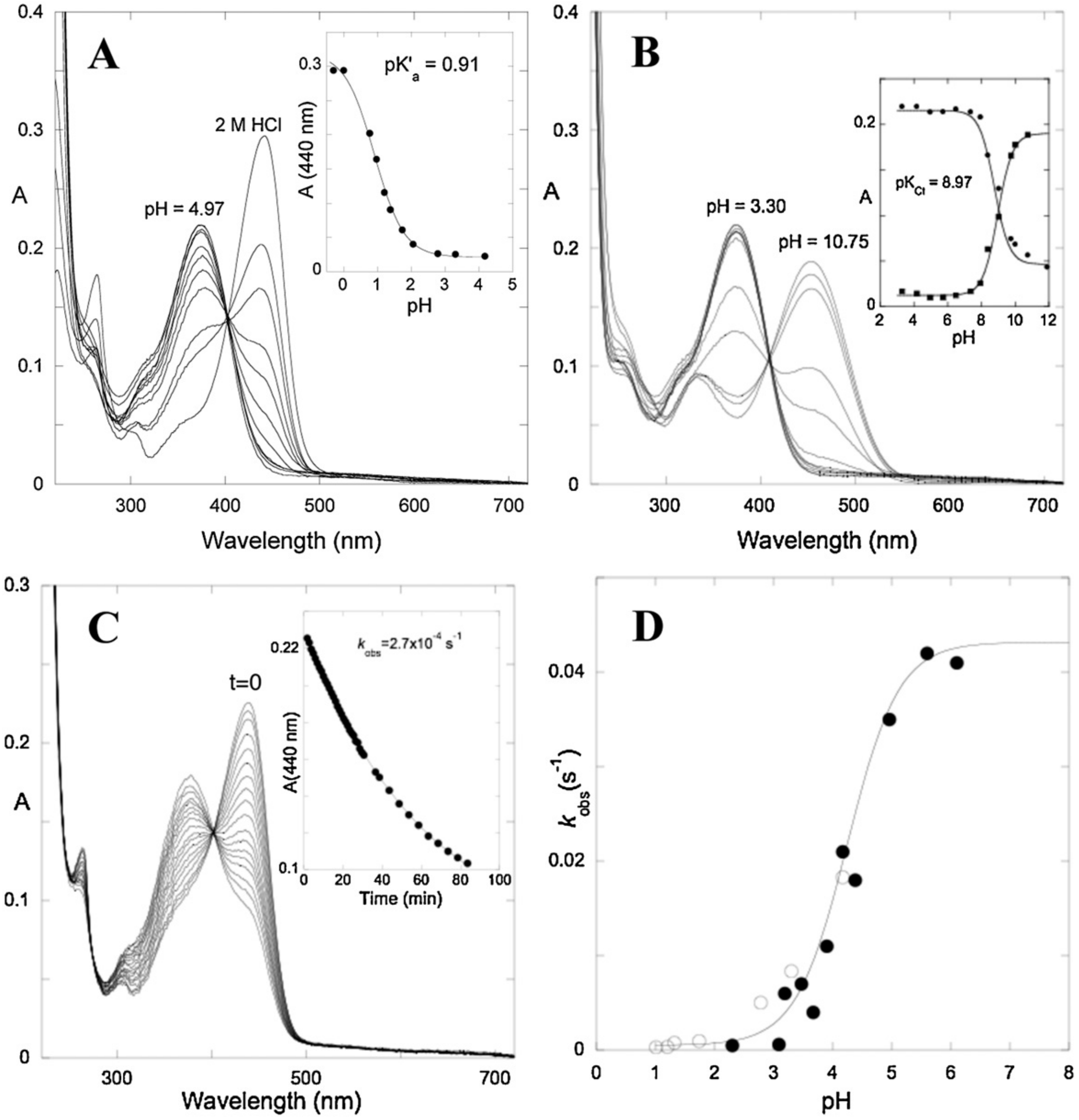

Fig. 1. Spectral variations of 3′-butoxy-7-methoxyflavylium 1.19×10^{-5} M in ethanol:water (30:70) upon direct pH jumps from a mother solution in 0.24 M HCl (ethanol:water, 30:70) to several pH values, after equilibration in the dark overnight. (A) 2 M HCl < pH < 4.97; inset: fitting of the absorption at 440 nm yields $pK'_a = 0.91$. (B) 3.30 < pH < 10.75; inset: simultaneous fitting of the absorbance at 377 nm (●) and 453 nm (■) leads to $pK_{Ct} = 8.97$. (C) Spectral variations over time upon at pH jump to pH 1.38; inset: fitting the kinetic trace at 440 nm as a monoexponential decay leads to $k_{obs} = 2.7(\pm 0.2) \times 10^{-4}$ s^{-1}. (D) pH dependence of k_{obs} determined from direct pH jumps (○) and from flash photolysis (●); fitting with Eq. (14) was achieved with $1.5(\pm 0.1) \times 10^{-6}/([H^+] + 3.4(\pm 0.2) \times 10^{-5}) + 1.25(\pm 0.1) \times 10^{-5}$.

spectral variations are compatible with an apparent acid–base type equilibrium, as reported in Eq. (5), involving the flavylium cation, **A**H$^+$, and *trans*-chalcone, **Ct**, with $pK'_a = 0.9(\pm 0.1)$. The assignment of the species with $\lambda_{max} = 377$ nm as the *trans*-chalcone was confirmed by ^{1}H NMR at pD = 3.5, through the large value of 15.8 Hz for the coupling constant between protons H3 and H4 (see Section 2) [30]. At higher pH values, **Ct** deprotonates to give unprotonated *trans*-chalcone, **Ct**$^-$, with $pK_{Ct} = 8.97(\pm 0.05)$, Fig. 1B.

Direct pH jumps from solutions of flavylium cation in 0.24 M HCl (ethanol:water, 30:70) to higher pH values, as shown in Fig. 1C, lead to spectral variations compatible with a first-order kinetic process where **A**H$^+$ disappears to give **Ct**. The rate of this process as a function of pH is shown in Fig. 1D, white circles. The shape of the curve is characteristic of a kinetic process controlled by the *cis*–*trans* isomerization [31]. In the same figure, the rate constants obtained from flash photolysis experiments where the recovery of **Ct** is measured after flash irradiation (see below) are also reported (black circles).

$$k_{obs} = \frac{K_h K_t}{[H^+] + K_h(1 + K_t)} k_i + k_{-i} \tag{14}$$

Considering Eqs. (2)–(4), the rate constant of *trans*-chalcone formation is given by Eq. (14) [2], used to fit the experimental data in Fig. 1D. The fitting was achieved for the values defined through Eqs. (15)–(17).

$$K_h K_t k_i = 1.5(\pm 0.1) \times 10^{-6}\ \text{M}^{-1}\,\text{s}^{-1} \tag{15}$$

$$K_h(1 + K_t) = 3.4(\pm 0.2) \times 10^{-5}\ \text{M}^{-1} \tag{16}$$

$$k_{-i} = 1.25(\pm 0.1) \times 10^{-5}\ \text{s}^{-1} \tag{17}$$

From the value of $K'_a = 10^{-0.91}$ (Fig. 1A) and subtracting Eq. (16) from Eq. (8), Eq. (18) is obtained (Eq. (8) for this compound has no K_a since there are no OH groups to form quinoidal base).

$$K_h K_t K_i = 0.12(\pm 0.02)\ \text{M}^{-1} \tag{18}$$

The ratio $K_h K_t K_i / K'_a = 0.99$ corresponds to the maximum of the mole fraction of **Ct** at the equilibrium confirming that [**CB**] ≈ [**Ct**] and the contribution of the other basic species is negligible. The ratio between Eqs. (15) and (18) confirms the value of k_{-i}.

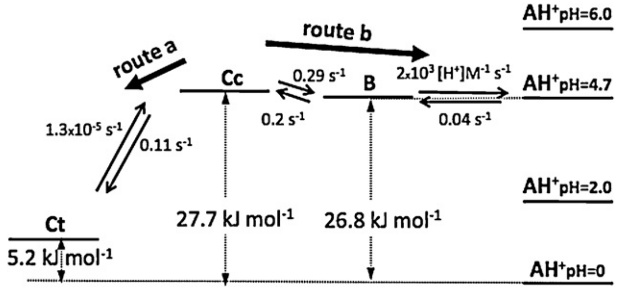

Scheme 2. Energy level diagram and rate constants for the compound 3′-butoxy-7-methoxyflavylium in ethanol:water, 30:70, at 294 K.

3.2. Photochemistry

Similarly to other flavylium chemical reaction networks, 3′-butoxy-7-methoxyflavylium is photochromic. The spectral variations upon continuous irradiation at 377 nm of the respective *trans*-chalcone at pH 2.0 is shown in Fig. 2. Flavylium cation is formed with a quantum yield of 0.1, and the system recovers thermally with a rate constant of $6(\pm 0.05) \times 10^{-4}\ \text{s}^{-1}$ (Fig. 2B).

More information regarding the system was obtained through flash photolysis experiments carried out at different pH values, as exemplified in Fig. 3 for pH 3.19 and pH 5.6. At pH 3.19, the flavylium absorption measured at 444 nm changes according to a bi-exponential law, the faster step accounting for an increase in absorbance immediately after the flash corresponding to the formation of **A**H⁺ from **Cc** via **B**, and the slower one consisting in a decrease on absorbance due to the thermal recovery of the system to give back **Ct**, the thermodynamically stable species at this pH value. On the other hand, the absorption changes of the *trans*-chalcone followed at 377 nm (Fig. 3A) show an initial bleaching occurring during the flash lifetime, an indication that **Ct** was consumed to give **Cc** [32], followed by a recovery of **Ct** also taking place through two kinetic steps, the faster corresponding to the formation of **Ct** from **Cc** and the slower consisting in the recovery of **Ct** from **A**H⁺. At pH 5.6, Fig. 3B, the formation of **A**H⁺ is almost imperceptible (top) and the trace at 377 nm (bottom) is nearly a monoexponential law. The values of the two rate constants of both bi-exponential processes, measured at 444 nm and 377 nm, are the same within experimental error (ca. 10%), see Figs. 4A and 1D for the pH dependence of the rate constants for the faster and for the slower steps, respectively.

The faster process can thus be assigned to the competition between two parallel reactions: a forward reaction to give **AH⁺** and a back reaction to recover **Ct**. Regarding the formation of **AH⁺**, a sequence of tautomerization and dehydration reactions should occur and the question is which of them is the rate determining step for flavylium formation after the flash. Anticipating the quantitative energy level diagram that could be drawn upon determination of the equilibrium (and kinetic) constants [33], the flash photolysis behaviour can be rationalized by Scheme 2.

The **Cc** species formed upon flash irradiation disappears via routes *a* plus *b* in Scheme 2 (parallel reactions). While the rate via route *a* is approximately equal to $k_i + k_{-i} \approx k_i$ ($k_i >> k_{-i}$), the rate via route *b* exhibits two potential dependences on pH: (i) the hydration reaction through the term $k_{-h}[\text{H}^+]$ and (ii) the tautomerization reaction due to the possibility of basic and acid catalysis, an effect previously reported by McClelland and co-workers and already observed in many flavylium systems [2,34]. Low pH values tend to favour formation of flavylium cation while at higher pH values **Ct** is completely recovered through route *a*.

The rate constants of the faster process determined from flash photolysis experiments carried out at several pH values are

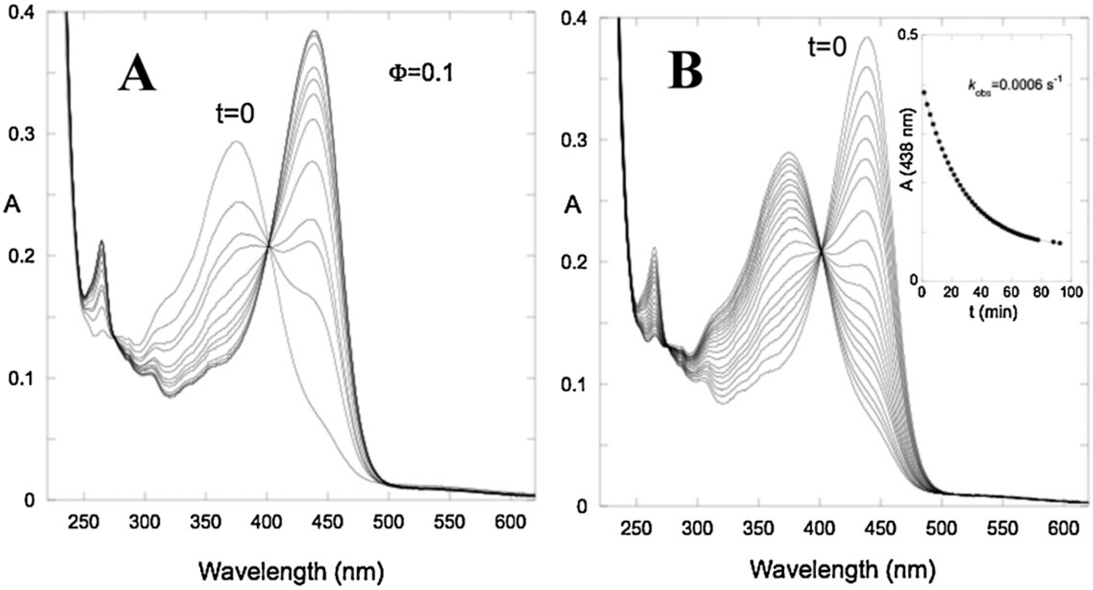

Fig. 2. (A) Spectral variations accompanying the irradiation at 377 nm of 3′-butoxy-7-methoxyflavylium at pH 2.0 (2 mL of solution, 2.06×10^{-5} M, ethanol:water, 30:70) for the following irradiation times: 0, 0.67, 1.33, 2, 3, 4, 5, 6, 7, 9, 11, 13, 15 min ($I_0 = 2.19 \times 10^{-7}$ Einstein min⁻¹). (B) Thermal recovery of the irradiated solution at 294 K; inset: fitting of the absorbance at 438 nm as a monoexponential decay leads to $k_{obs} = 6.0(\pm 0.05) \times 10^{-4}\ \text{s}^{-1}$.

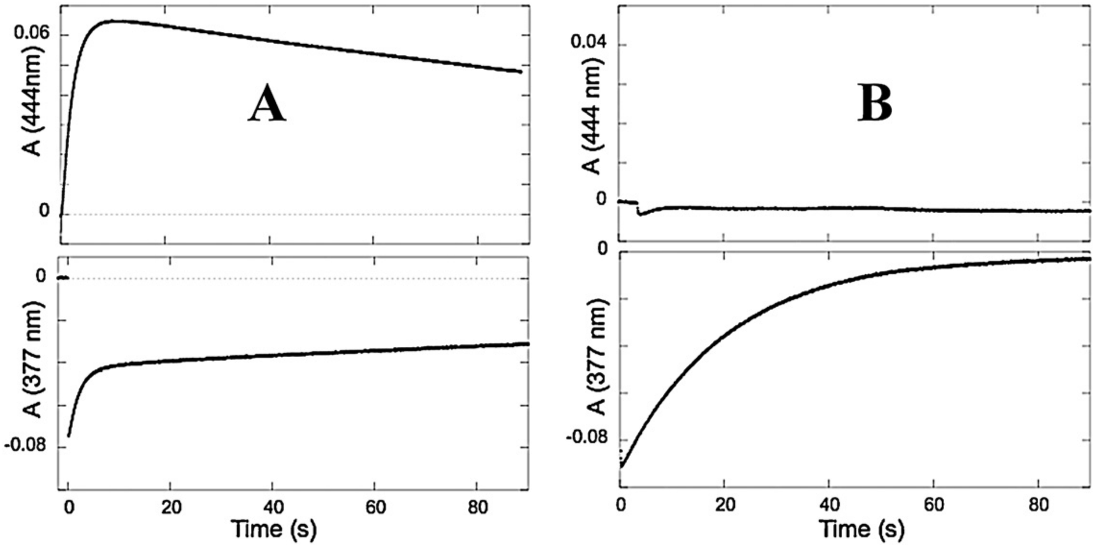

Fig. 3. Flash photolysis of 3′-butoxy-7-methoxyflavylium 2.74×10^{-5} M in ethanol:water, 30:70 at pH 3.19 (A) and at pH 5.6 (B).

presented in Fig. 4. Inspection of these plots suggests a change of regime on the pH dependence of route *b* (the contribution of route *a* for k_{obs} is pH independent) with k_{obs} increasing with increasing pH until pH ≈ 3.7 and decreasing thereon. At low pH values, the hydration is expected to be relatively fast (it is proportional to [H$^+$]) and the kinetics is controlled by the tautomerization reaction. The small increase of the tautomerization rate can be attributed to a basic catalysis [34] (no acidic catalysis was detected in this pH range, otherwise an increase of the rate would be expected at low pH values). However, at higher pH values the hydration rate decreases and becomes the rate-determining step. In conclusion, the rate constants for the branch controlled by the tautomerization reaction should follow Eq. (19) while the branch controlled by the hydration reaction should follow Eq. (20). In Eq. (19), it was considered that since the hydration is fast, once **B** is formed it immediately transforms into **A**H$^+$ and no reversibility from **B** to **Cc** was included. On the other hand, in Eq. (20) it was considered that **B** and **Cc** have time to (pseudo) equilibrate before the hydration occurs [2].

$$k_{obs(Taut)} = k_i + k_{-t} + k_{-t}^{OH}[OH^-] \tag{19}$$

$$k_{obs(Hyd)} = \frac{k_i K_t}{1 + K_t} + k_h + \frac{k_{-h}[H^+]}{1 + K_t} \tag{20}$$

Fitting of the data in Fig. 4A was achieved by means of Eq. (19) with $k_i + k_{-t} = 0.4\ s^{-1}$ and $k_{-t}^{OH} = 2.5(\pm 0.3) \times 10^9\ M^{-1}\ s^{-1}$ (tautomerization control) and Eq. (20) with $k_i K_t/(1 + K_t) + k_h = 0.085\ s^{-1}$ and $k_{-h} = 2.0(\pm 0.3) \times 10^3\ M^{-1}\ s^{-1}$ (hydration control).

In order to confirm this interpretation, the pH dependent mole fraction of flavylium cation formed after the first kinetic step upon flash irradiation was calculated using the kinetic traces at 377 and 444 nm for each pH (Fig. 3) and are shown in Fig. 4B. The mole fraction of flavylium cation was calculated

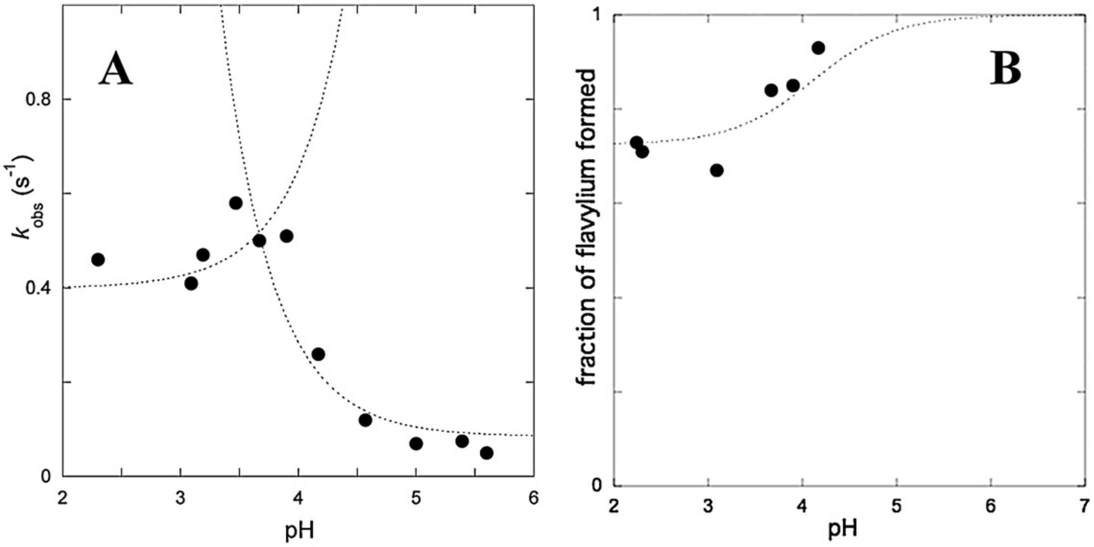

Fig. 4. (A) Observed rate constants for the faster process upon flash irradiation as a function of pH; fitting for the tautomerization control range (pH < 3.7) attained through Eq. (19) with $0.4(\pm 0.1) + 2.5(\pm 0.3) \times 10^9[OH^-]$ and for the hydration control range (pH > 3.7) attained through Eq. (20) with $0.04 + 2.0(\pm 0.2) \times 10^3[H^+]$. (B) Mole fraction of the flavylium cation after the first kinetic step upon flash irradiation as a function of pH; fitting achieved with Eq. (21) for $(0.29(\pm 0.1) + 2.5(\pm 0.3) \times 10^9[OH^-])/(0.4(\pm 0.1) + 2.5(\pm 0.3) \times 10^9[OH^-])$.

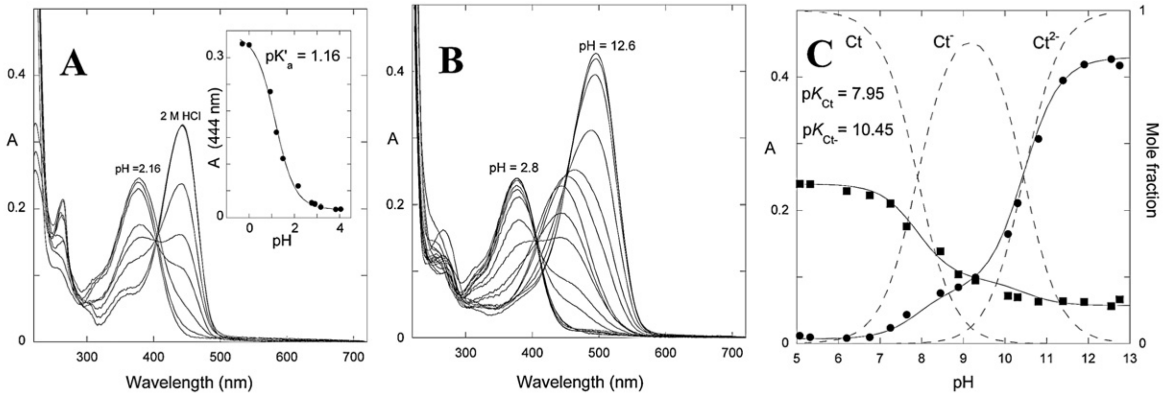

Fig. 5. Spectral variations of 3′-butoxy-7-hydroxyflavylium 1.1×10^{-5} M in ethanol:water (30:70) upon direct pH jumps from a mother solution in 0.24 M HCl (ethanol:water, 30:70) to several pH values, after equilibration in the dark overnight. (A) 2 M HCl < pH < 2.16; inset: fitting of the absorption at 444 nm yields $pK'_a = 1.16(\pm 0.08)$. (B) 2.76 < pH < 12.55. (C) Simultaneous fitting of the absorbance at 495 nm (●) and 377 nm (■) over the pH range in (B) leads to $pK_{Ct} = 7.95(\pm 0.1)$ and $pK_{Ct^-} = 10.45(\pm 0.1)$; traced lines correspond to the mole fraction distribution of the *trans*-chalcone species.

as $\chi_{AH^+} = [AH^+]/[Ct]_0$ with $[AH^+] = A_{444}/\varepsilon_{444}(AH^+)$ and $[Ct]_0 = A^0_{377}/\varepsilon_{377}(Ct)$, considering $b = 1$ cm. The value of A_{444} was obtained from the respective kinetic trace after the first kinetic process, the value of A^0_{377} from the respective kinetic trace at $t = 0$ (immediately after the flash), $\varepsilon_{444}(AH^+) = 24{,}740\ M^{-1}\ cm^{-1}$ and $\varepsilon_{377}(Ct) = 17{,}870\ M^{-1}\ cm^{-1}$ (Fig. 1A).

Fitting of the data in Fig. 4B was made with Eq. (21) that accounts for the fraction of flavylium cation obtained under tautomerization control. In the case of the hydration control, the system essentially reverts back to **Ct** and the separation between the slow process upon flash irradiation and the thermal recovery cannot be made with sufficient accuracy from the traces at 377 nm.

$$\chi_{AH^+} = \frac{k_{-t} + k^{OH}_{-t}[OH^-]}{k_i + k_{-t} + k^{OH}_{-t}[OH^-]} \tag{21}$$

The fitting was achieved using the values of $k^{OH}_{-t} = 2.5 \times 10^9\ M^{-1}\ s^{-1}$ and $k_i + k_{-t} = 0.4\ s^{-1}$ determined above, allowing to obtain $k_{-t} = 0.29\ s^{-1}$ and consequently $k_i = 0.4 - 0.29 = 0.11\ s^{-1}$.

Substitution of k_i in Eq. (15) permits to obtain

$$K_h K_t = 1.36 \times 10^{-5}\ M^{-1} \tag{22}$$

Substitution of Eq. (22) in Eq. (16) gives $K_h = 2.0 \times 10^{-5}\ M^{-1}$ and from Eq. (22), $K_t = 0.69$, leading to $k_t = 0.2\ s^{-1}$; Eqs. (18) and (22) allow to obtain $K_i = 8.8 \times 10^4$.

In conclusion, the data obtained from direct pH jumps and flash photolysis can be fitted with the same set of constants presented in Table 1.

3.3. 3′-Butoxy-7-hydroxyflavylium

The pH dependent spectral variations of dark equilibrated solutions of 3′-butoxy-7-hydroxyflavylium (ethanol:water, 30:70) are shown in Fig. 5A for a more acidic region (2 M HCl < pH < 2.16) and in Fig. 5B for a larger pH range (2.8 < pH < 12.6).

Fitting the data for the more acidic region in Fig. 5A leads to $pK'_a = 1.16(\pm 0.08)$. The data is compatible with an equilibrium between the flavylium cation and a species exhibiting an absorption band which shape and position is characteristic of the *trans*-chalcone, **Ct**. This interpretation was corroborated by ^1H NMR where **Ct** is clearly identified by the large coupling constant (15.6 Hz) between protons H3 and H4 (see Section 2).

In Fig. 5B, the spectral variations show red-shits compatible with successive formation of unprotonated *trans*-chalcones, **Ct**$^-$ and **Ct**$^{2-}$. Simultaneous fitting of the absorbances at 377 and 495 nm leads to $pK_{Ct} = 7.95(\pm 0.1)$ and $pK_{Ct^-} = 10.45(\pm 0.1)$, Fig. 5C.

Unlike the previous flavylium, 3′-butoxy-7-hydroxyflavylium has a OH group in position 7 allowing the formation of a quinoidal base upon deprotonation. Determination of the pK_a was achieved by means of stopped-flow experiments, Fig. 6. Solutions of flavylium cation (0.24 M HCl in ethanol:water, 30:70) were submitted to pH jumps to higher pH values and the absorbance measured immediately after (dead time of the stopped-flow lower than 10 ms). The absorbance variations as a function of pH are compatible with an acid–base equilibrium between flavylium cation and quinoidal base, Eq. (1), with $pK_a = 4.6(\pm 0.1)$, see inset in Fig. 6A.

The kinetics of direct pH jumps is exemplified for final pH values of 6.75 and 12.55 in Fig. 6B and C, respectively. In Fig. 6B, the quinoidal base evolves to the *trans*-chalcone **Ct**, while in Fig. 6C the same quinoidal base leads to the ionized *trans*-chalcone **Ct**$^{2-}$ ($\lambda_{max} = 495$ nm). This procedure was extended to cover the pH

Table 1
Thermodynamic and kinetic constants of 3′-butoxy-7-methoxyflavylium.[a]

pK'_a	K_h (M^{-1})	K_t	K_i	k_i (s^{-1})	k_{-i} (s^{-1})	k_t (s^{-1})	k_{-t} (s^{-1})	k_h (s^{-1})	k_{-h} ($M^{-1}\ s^{-1}$)	k^{OH}_{-t} ($M^{-1}\ s^{-1}$)
0.9	2.0×10^{-5}	0.69	8.8×10^3	0.11	1.25×10^{-5}	0.2	0.29	0.04	2.05×10^3	2.5×10^9

[a] Estimated error is about 10%.

Table 2
Rate and equilibrium constants of 3′-butoxy-7-hydroxyflavylium obtained from Figs. 5 and 6.

$pK'_a{}^{(1)}$	$pK_a{}^{(2)}$	$K_h K_t K_i{}^{(2)}$	$k_h{}^{(2)}$	$k_{-i}{}^{(2)}$	$K_h K_t k_i{}^{(2)}$	$K_t k_i/k_{-h}{}^{(2)}$
1.2	4.6	$0.063\ M^{-1}$	$0.023\ s^{-1}$	$5.7 \times 10^{-5}\ s^{-1}$	$4.0 \times 10^{-6}\ s^{-1}\ M^{-1}$	1.9×10^{-4} M

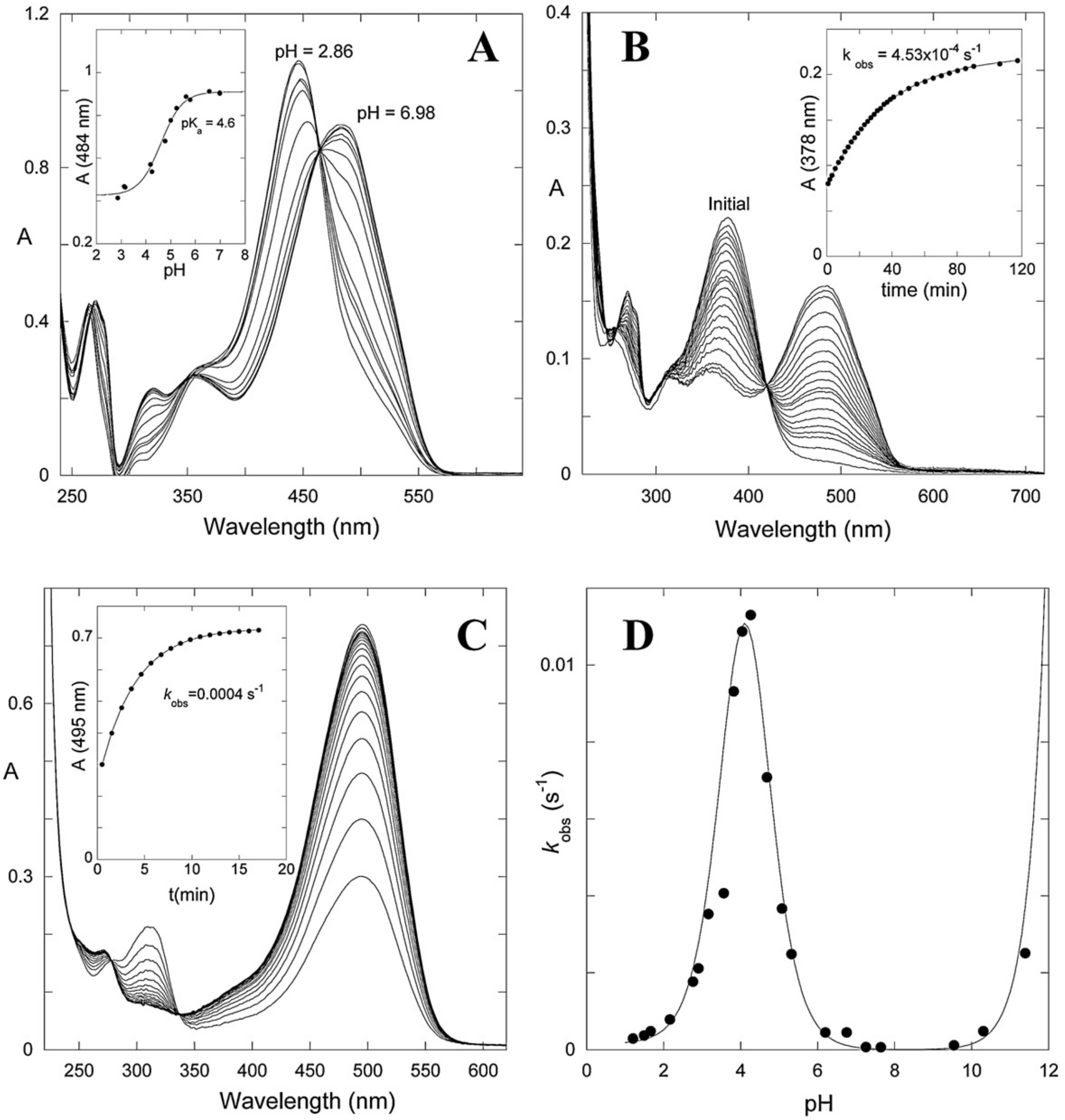

Fig. 6. (A) Spectral variations of 3′-butoxy-7-hydroxyflavylium 5.43×10^{-5} M in ethanol:water (30:70) upon direct pH jumps from a mother solution in 0.24 M HCl (ethanol:water, 30:70) to several pH values in the range $2.86 < \text{pH} < 6.98$, followed by stopped-flow (dead time ca. 10 ms); inset: fitting of the absorption at 484 nm yields $pK_a = 4.6(\pm 0.1)$. (B) Spectral variations over time upon at pH jump to pH 6.75; inset: fitting the kinetic trace at 378 nm as a monoexponential decay leads to $k_{obs} = 4.53(\pm 0.05) \times 10^{-4}\ s^{-1}$. (C) Same as in B to pH 6.75; inset: fitting the kinetic trace at 495 nm as a monoexponential decay leads to $k_{obs} = 4.0(\pm 0.1)\ x10^{-4}\ s^{-1}$. (D) pH Dependence of k_{obs} determined from direct pH jumps; fitting with Eq. (23) for $pK_a = 4.6(\pm 0.1)$, $K_h K_t k_i = 4.0 \times 10^{-6}\ s^{-1}$ M, $K_t k_i / k_{-h} = 1.9 \times 10^{-4}$ M, $k_{-i} = 5.7 \times 10^{-5}\ s^{-1}$ and $k^{OH} = 1.5(\pm 0.4)\ s^{-1}\ M^{-1}$.

range 1–12, the respective observed rate constants being reported in Fig. 6D. A bell-shaped curve is obtained in acidic medium and a linear dependence with $[OH^-]$ concentration occurs in basic medium, following Eq. (23).

$$k_{obs} \frac{([H^+]/([H^+] + K_a))K_h K_t k_i + k_{-i}[H^+]}{((K_t k_i)/k_{-h}) + [H^+]} + k^{OH}[OH^-] \tag{23}$$

The bell shaped part of Eq. (23) is obtained considering the kinetic scheme shown in Eq. (24).

$$\mathbf{Ct} \underset{(K_t/(1+K_t))k_i}{\overset{k_{-i}}{\rightleftharpoons}} \mathbf{Cc} \rightleftharpoons \mathbf{B} \underset{(([H^+])/([H^+ + K_a]))k_h}{\overset{k_{-h}/(1+K_t)}{\rightleftharpoons}} \mathbf{A}H^+ \rightleftharpoons \mathbf{A} + \mathbf{H}^+ \tag{24}$$

In this scheme, the equilibrium between **B** and **Cc** is considered to be much faster than the other processes, except the acid–base equilibrium **AH**$^+$/**A**, which is the fastest process of the network. At lower pH values, the system is kinetically controlled by the *cis–trans* isomerization while at higher pH values the hydration is the rate-determining step. In basic medium, the direct attack of OH^- to the base leads to the ionized *cis*-chalcones that isomerize to form the respective ionized *trans*-chalcones. Fitting of the data in Fig. 6D was obtained for the constants reported in Table 2.

As in the case of the previous compound, irradiation of the **Ct** species of 3′-butoxy-7-hydroxyflavylium leads to formation of flavylium cation, in this case with $\Phi = 0.05$, Fig. 7A. The thermal recovery from **Ct** back to the flavylium occurs with $k_{obs} = 4(\pm 0.1) \times 10^{-4}\ s^{-1}$ at pH 2.0.

3.4. Flash photolysis

The flash photolysis traces represented in Fig. 8 regard the formation and disappearance of flavylium cation after the

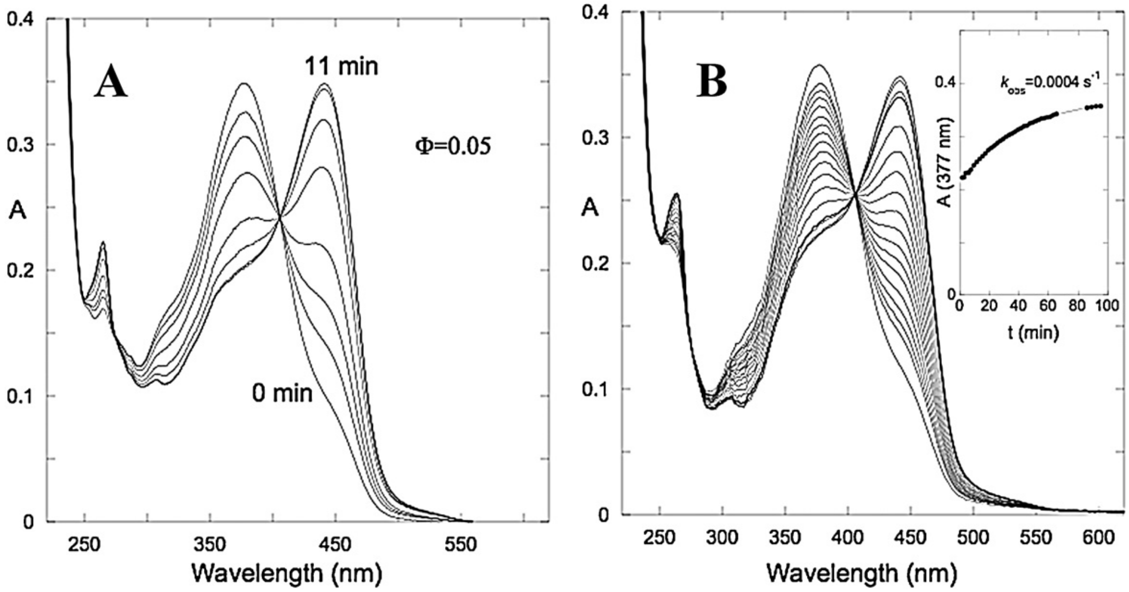

Fig. 7. (A) Spectral variations accompanying the irradiation at 377 nm of 3′-butoxy-7-hydroxyflavylium at pH 2.0 (2 mL of solution, 1.91×10^{-5} M, ethanol:water, 30:70) for the following irradiation times: 0, 0.5, 1, 2.5, 5, 7, 9, 11 min ($I_0 = 2.19 \times 10^{-7}$ Einstein min^{-1}). (B) Thermal recovery of the irradiated solution at 294 K; inset: fitting of the absorbance at 438 nm as a monoexponential decay leads to $k_{obs} = 4.0(\pm 0.1) \times 10^{-4}$ s^{-1}.

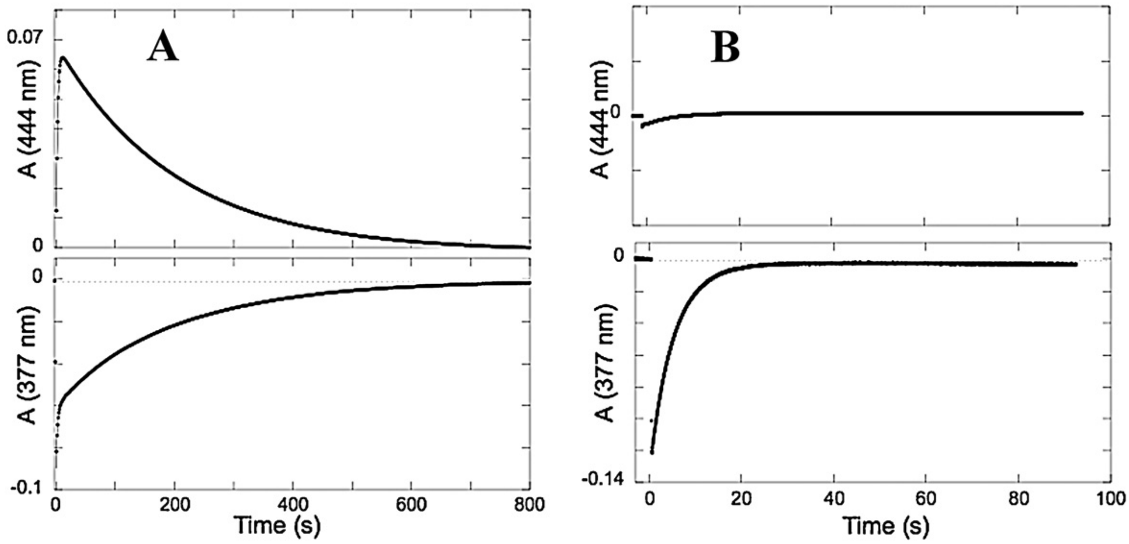

Fig. 8. Flash photolysis of 3′-butoxy-7-hydroxyflavylium 3.3×10^{-5} M in ethanol:water, 30:70 at pH 4.09 (A) and at pH 6.2 (B).

flash (444 nm) and the bleaching and recovery of the *trans*-chalcone (377 nm). At pH 4.09, both traces are fitted with two exponentials with the same lifetimes, $k_{obs1} = 0.4(\pm 5\%)$ s^{-1} and $k_{obs2} = 0.005(\pm 5\%)$ s^{-1}, while at pH 6.2 the data is suitably fitted by a single exponential with $k_{obs} = 0.2$ s^{-1}. The rate constants for the faster process are plotted as a function of pH in Fig. 9A while those of the slower process follow the bell shaped pH dependence shown in Fig. 6D. The behaviour is qualitatively similar to that of the previous flavylium compound.

When the kinetics is controlled by the tautomerization Eqs. (19) and (21) are still valid, but when hydration is the rate-determining step equilibration of flavylium cation with quinoidal base introduces reversibility through the hydration constant and Eq. (20) should be substituted by Eq. (25)

$$k_{obs1} = \frac{k_i K_t}{1 + K_t} + k_h \frac{[\mathrm{H}^+]}{[\mathrm{H}^+] + K_a} + k_{-h}[\mathrm{H}^+] \qquad (25)$$

As in the previous example of the methoxyflavylium analogous the flash photolysis allows to obtain all the rate and equilibrium

Table 3
Rate and equilibrium constants of 3′-butoxy-7-hydroxyflavylium.

pK_a	K_h (M^{-1})	K_t	K_i	k_h (s^{-1})	k_{-h} (s^{-1})	k_t (s^{-1})	k_{-t} (s^{-1})	k_i (s^{-1})	k_{-i} (s^{-1})
4.6	1.9×10^{-5}	0.16	1.4×10^4	0.02	1.1×10^3	0.07	0.31	0.89	6.4×10^{-5}

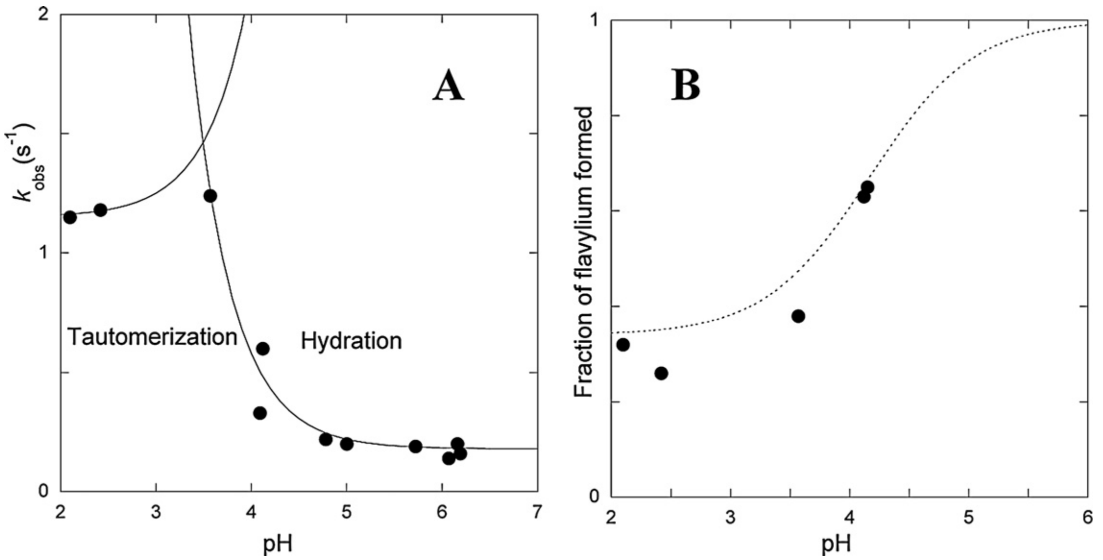

Fig. 9. (A) Observed rate constants for the faster process upon flash irradiation of solutions of 3′-butoxy-7-hydroxyflavylium as a function of pH; fitting for the tautomerization control range (pH < 3.5) attained through Eq. (19) with $1.2 + 1.0 \times 10^{10}[OH^-]$ and for the hydration control range (pH > 3.5) attained through Eq. (25) with $0.17 + (0.023[H^+])/([H^+] + 2.5(\pm 0.3) \times 10^{-5}) + 1.0(\pm 0.5) \times 10^{10}[H^+]$. (B) Mole fraction of the flavylium cation after the first kinetic step upon flash irradiation as a function of pH; fitting achieved with Eq. (21) for $(0.31 + 1.0(\pm 0.5) \times 10^{10}[OH^-])/(1.2 + 1.0 \times 10^{10}[OH^-])$.

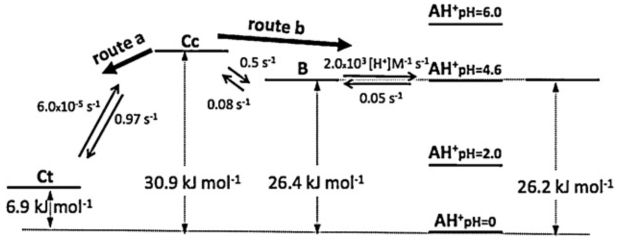

Scheme 3. Energy level diagram and rate constants for the compound 3′-butoxy-7-hydroxyflavylium in ethanol:water, 30:70, at 294 K.

constants of the system. Regarding the tautomerization control the limits of Eq. (19) at lower pH values and (21) are respectively $k_i + k_{-t} = 1.2\,\mathrm{s}^{-1}$ and $k_{-t}/(k_i + k_{-t}) = 0.26$, leading to $k_i = 0.89\,\mathrm{s}^{-1}$ and to $k_{-t} = 0.31\,\mathrm{s}^{-1}$.

The fitting of Fig. 9A is well defined and according to Eq. (25) should be given by $k_i K_t/(1 + K_t) = 0.17$, which allows to calculated $K_t = 0.23(\pm 0.05)$ substitution of K_t in 3rd column of Table 2 leads to $K_h K_i = 0.27\,\mathrm{M}^{-1}$. Substitution of k_i in 6th column of Table 2 gives $K_h K_t = 4.4 \times 10^{-6}\,\mathrm{M}^{-1}$ and $K_h = 1.9 \times 10^{-5}\,\mathrm{M}^{-1}$ and $K_i = 1.4 \times 10^4$ and thus k_{-i} and k_t are obtained.

A reasonable fitting of the fraction of flavylium cation formed after the flash using Eq. (21) and the data from Table 3 is shown in Fig. 9B.

The energy level diagram for this compound is shown in Scheme 3.

4. Conclusions

Flash photolysis is an excellent technique to complement the pH jumps commonly used in the study of the photochromic flavylium compounds network of chemical reactions. Conjugation of the two techniques allows calculation of all the kinetic and thermodynamic constants of the system and this information is conveniently presented in an energy level diagram. The rate of *trans*-chalcone appearance from flavylium cation upon a pH jump is not only a function of the *cis–trans* isomerization barrier, but also of the fraction of *cis*-chalcone available to isomerize; slow appearance of **Ct** could result from the low isomerization rate or from the small fraction of **Cc** available to isomerize, as reported for 3′-butoxyflavylium derivatives.

Acknowledgments

This work was supported by Fundação para a Ciência e Tecnologia, National NMR Network, project PTDC/QUI-QUI/117996/2010, Post-doc grant SFRH/BPD/18214/2004 (VP).

References

[1] J.C. Crano, R.J. Guglielmetti (Eds.), Organic Photochromic and Thermochromic Compounds, vol. 1, Plenum Press, NY, 1999.
[2] F. Pina, M.J. Melo, C.A.T. Laia, A.J. Parola, J.C. Lima, Chemical Society Reviews 41 (2012) 869–908.
[3] F. Pina, M.J. Melo, A.J. Parola, M. Maestri, V. Balzani, Chemistry A: European Journal 4 (1998) 2001–2007.
[4] J.G. Sweeny, G.A. Iacobucci, Journal of Agricultural and Food Chemistry 31 (1983) 531–533.
[5] P. Coggon, G.A. Moss, H.N. Graham, G.W. Sanderson, Journal of Agricultural and Food Chemistry 21 (1973) 727–733.
[6] R. Brouillard, G.A. Iacobucci, J.G. Sweeny, Journal of the American Chemical Society 104 (1982) 7585–7590.
[7] M.J. Melo, S. Moura, A. Roque, M. Maestri, F. Pina, Journal of Photochemistry and Photobiology A: Chemistry 135 (2000) 33–39.
[8] L. Jurd, USA Patent 3301683.
[9] J.S. Buck, I.M. Heilbron, Journal of the Chemical Society 123 (1923) 2521–2531.
[10] D. Amic, N. Trinajstic, D.D. Amic, Journal of the Chemical Society: Perkin Transactions 2 (11) (1992) 1933–1938.
[11] R. Gomes, A.M. Diniz, A. Jesus, A.J. Parola, F. Pina, Dyes and Pigments 81 (2009) 69–79.
[12] A.M. Diniz, R. Gomes, A.J. Parola, C.A.T. Laia, F. Pina, Journal of Physical Chemistry B 113 (2009) 719–727.
[13] M. Elhabiri, P. Figueiredo, F. George, J.-P. Cornard, A. Fougerousse, J.-C. Martin, R. Brouillard, Canadian Journal of Chemistry 74 (1996) 697–706.
[14] R. Gavara, V. Petrov, F. Pina, Photochemical and Photobiological Sciences 9 (2010) 298–303.
[15] H. Horiuchi, A. Tsukamoto, T. Okajima, H. Shirase, T. Okutsu, R. Matsushima, H. Hiratsuka, Journal of Photochemistry and Photobiology 205 (2009) 203–209.
[16] R. Brouillard, B. Delaporte, Journal of the American Chemical Society 99 (1977) 8461–8468.
[17] R. Brouilard, B. Delaporte, J.-E. Dubois, Journal of the American Chemical Society 100 (1978) 6202–6205.
[18] F. Pina, Journal of the Chemical Society: Faraday Transactions 94 (1998) 2109–2116;
(Correction in Scheme 1 see) F. Pina, Journal of the Chemical Society: Faraday Transactions 94 (1998) 3781.

[19] F. Pina, M.J. Melo, M. Maestri, R. Ballardini, V. Balzani, Journal of the American Chemical Society 119 (1997) 5556–5561.

[20] F. Galindo, J.C. Lima, S.V. Luis, A.J. Parola, F. Pina, Advanced Functional Materials 15 (2005) 541–545.

[21] F. Pina, T.A. Hatton, Langmuir 24 (2008) 2356–2364.

[22] F. Pina, J.C. Lima, A.J. Parola, C.A.M. Afonso, Angewandte Chemie: International Edition 43 (2004) 1525–1527.

[23] F. Pina, M.J. Melo, M. Maestri, P. Passaniti, V. Balzani, Journal of the American Chemical Society 122 (2000) 4496–4498.

[24] According to our previous experience this is a convenient situation to a good performance of the photochromic system.

[25] F.W. Küster, A. Thiel, Tabelle per le Analisi Chimiche e Chimico-Fisiche, 12th ed., 1982, Hoepli, Milano, pp. 157–160. The universal buffer used was prepared in the following way: 2.3 cm^3 of 85% (w/w) phosphoric acid, 7.00 g of monohydrated citric acid, and 3.54 g of boric acid are dissolved in water; 343 mL of 1 M NaOH is then added, and the solution diluted to 1 dm^3 with water.

[26] C.G. Hatchard, C.A. Parker, Proceedings of the Royal Society of London Series A 235 (1956) 518–536.

[27] M. Maestri, R. Ballardini, F. Pina, M.J. Melo, Journal of Chemical Education 74 (1997) 1314–1316.

[28] A. Ravikrishnan, P. Sudhakara, P. Kannan, Polymer Degradation and Stability 93 (2008) 1564–1570.

[29] K. Takeuchi, M.R. Jirousek, M. Paal, G. Ruhter, T. Schotten, US2004009976-A1 (2004).

[30] A. Roque, J.C. Lima, A.J. Parola, F. Pina, Photochemical and Photobiological Sciences 6 (2007) 381–385.

[31] F. Pina, V. Petrov, C.A.T. Laia, Dyes and Pigments 92 (2011) 877–889.

[32] In flavylium systems, the Cc species usually shows a smaller mole absorption coefficient than Ct.

[33] Considering $DG = -RT\ln K$.

[34] R.A. McClelland, S. Gedge, Journal of the American Chemical Society 102 (1980) 5838–5848.